Micromechanism of High-temperature Fatigue Properties of Inconel 718 Nickel-based Alloy Treated by Laser Peening

Jie Sheng[1,2], Huixia Liu[3], Youyu Lin[2], Kai Liu[2], Guoyang Zhou[2], Yang Wang[2], Emmanuel Agyenim-Boateng[4], and Shu Huang[3*]

[1]School of Materials Science and Engineering, Jiangsu University, 301 Xuefu Road, Zhenjiang 212013, China
[2]Jiangsu SUMEC Hardware & Tools Co., Ltd., 1 Xinghuo Road, Nanjing 210032, China
[3]School of Mechanical and Engineering, Jiangsu University, 301 Xuefu Road, Zhenjiang, 212013, China
[4]Department of Agricultural Engineering, University of Cape Coast, 1 School Bus Road, Cape Coast , Ghana
[*]Corresponding author's e-mail: huangshu11@sina.com

The fatigue lives of IN718 alloy treated by laser peening (LP) were examined at high temperature. The microstructural response of the fatigue specimens was revealed. The results show that LP can refine the grain size, and produce new dislocation structures. The mechanical twins in the high-power LPed specimens can interact with other dislocations to refine the grains. A special "dislocation-pre-cipitate" entanglement in the high-temperature fatigue LPed specimens at 700 °C was helpful to form a more effective pinning effect on the dislocation movement and thus preventing the initiation and propagation of fatigue cracks.

1. Introduction

Inconel 718 nickel-based alloy (IN718 alloy) is widely used in aeroengine manufacturing industry, owning to its good oxidation resistance, corrosion resistance and high-temperature fatigue properties [1-3]. However, the fatigue failure still occurs in advance for the IN718 alloy parts under thermal-mechanical loading while working under ultimate temperature and high loading [4]. The research on the fatigue properties of superalloy under high temperature and high loading has always been a hot topic [5-7]. In order to reveal the mechanism of high-temperature fatigue failure of IN718 alloy, many researches have been carried out on the fatigue properties of IN718 alloy [8-13]. It is worth noting that the microstructural characteristics have a very important influence on the fatigue crack growth behavior of IN718 alloy. It is well known that the main element of matrix in IN718 alloy is Ni while the main strengthening phase is γ"-precipitate. However, IN718 can only work at a certain range of temperature (-253 °C－700 °C). With the increase of service temperature(＞700 °C), the metastable γ"-precipitate will gradually coarsen and lose the coherent relationship with the matrix. As a result, γ"-precipitate can transform to δ-precipitate. The δ-precipitate is brittle. Hence, the ductility and other mechanical properties of IN718 alloy are reduced in a specific high-temperature environment. In addition, the effect of grain morphology on the properties of materials is also worthy of attention [14]. Schlesinger et al [15] analyzed the low-cycle thermo-mechanical fatigue crack growth behavior of IN718 by replica method. They discussed the mechanism of low-cycle thermo-mechanical fatigue-damage and the orientation of failure grain boundary in the region where secondary cracks occurred. The results showed that fatigue cracks mainly propagated in the mode of transgranular, accompanied by local intergranular propagation, and the grains with consistent lattice and grain boundary were not easy to appear intergranular failure than the randomly oriented grains. Therefore, it is a feasible method to improve the properties of IN718 alloy at high temperature by changing its original microstructures. It's of great importance to find a proper technology to improve the fatigue properties of IN718 alloy by changing the microstructures.

LP is a special high-energy peening technology, which uses laser-induced shock wave to produce plastic deformation on the surface of the material, leading to the formation of high amplitude compressive residual stress(CRS) and strengthening structure that contribute to improve the corrosion resistance, wear resistance and fatigue resistance [16-21]. The depth of the CRS affected layer is 3−4 times that of the traditional mechanical shot peening. The LP-induced CRS inhibits the initiation and propagation of surface cracks by changing the stress state of the material surface. Many previous studies have shown that LP is of great help to improve the mechanical properties and fatigue resistance of material [22-24]. But what is more worthy of our attention is that LP can change the microstructure of material. Because of the plastic deformation layer induced on the surface of material by LP, more uniform, dense and stable nanocrystals and dislocation entanglements can be generated on the material surface, which is helpful to improve the stability of high-temperature fatigue characteristics of LP process [25-26]. Gill et al [27] exhibited that LPed specimens showed an increase in near-surface low angle misorientations (<15°), indicating the extent plastic deformation introduced by shock wave. In addition, LP induced high dislocation density in the near-surface of IN718 alloy. Telang et al [28] also found high dislocation density as well as deformation induced twins in the IN718 alloy due to high strain rates (~10^6

s^{-1}) of the LP process. Kattoura et al [29] believed that the severe surface plastic deformation due to LP treatment altered the microstructures of the surface layer of material. The LP process induces an extreme increase in dislocation density causing formation of dislocation entanglements and slip bands. These changes caused high surface hardening. By using the technique of Electron Backscattered Diffraction(EBSD), it was confirmed that LP also significantly refines the grains in the surface layer leading to a grain size gradient structure. Crystal defects, such as high-density dislocation, dislocation tangles, dislocation cells, dislocation arrays, twins, dislocation walls, stacking faults and subgrains, are produced by LP in the LPed IN718 alloy. These crystal defects are proved to provide nucleation sites for γ', γ″ and δ-precipitate [30]. Our previous work showed a new formed substructure of submicron rhombic blocks with lengths in the range of 400-600 nm in the LP treated specimens, which are beneficial for the stability of mechanical properties at high temperature [3].

The above researches have focused on the microstructural changes of IN718 alloy treated by LP at room temperature. But the coupled service environment of cyclic loading and high temperature is very complex, and IN718 alloy has a very special strengthening structure. It is still unclear that how the microstructure of LP induced ultra-high strain-rate changes under the condition of high-temperature cyclic loading. In addition, how the interaction of the high-temperature precipitates and dislocation affect the plastic deformation of IN718 alloy also need further research.

In this study, the microstructural response of IN718 alloy specimens treated by LP at different laser power densities and different service temperatures are systematically researched, and the evolution of microstructures and the interaction between microstructures and precipitates are also explored.

2. Material and experiments

2.1 Experimental material

The IN718 alloy was solution treated at 900 ℃ for 1 h, water quenched and then aged at 700 ℃ for 6 h, furnace cooled to 600 ℃ and aged at 600 ℃ for 8 h followed by air cooling. The specimens were cut into a dog-bone shape as shown in Fig.1. The chemical composition of IN718 alloy is shown in Table 1. Prior to the LP treatment, the surface of the specimens were polished with SiC paper first, then cleaned in deionized water. After that, ultrasound in ethanol was used to degrease the specimen surface, and then stored in a drying oven.
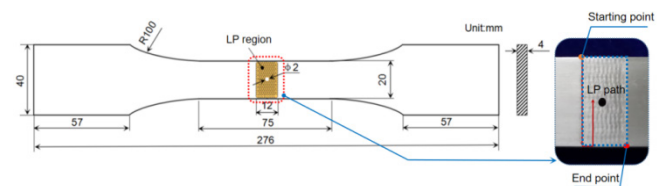
Fig.1 Dimension of LPed specimens and sketch of LP path.

Table 1 Chemical composition of IN718

Chemical composition (Wt./%)	Ni	Cr	C	Si	Mn	S	P	Al
	52.50	19.25	0.058	0.149	0.165	0.001	0.011	0.44
Chemical composition (Wt/.%)	Cu	Ti	Mo	B	Nb+Ta	Co	Fe	
	0.044	1.10	2.98	0.003	4.93	0.135	Remainder	

2.2 Principle and experimental procedure of LP

A GAIA Nd:YAG laser machine(Thales Laser Ltd.) was used to conduct the LP processing. A pulse width of 15 ns and a wavelength of 1064 nm were adopted during the processing while a repetition rate of 1 Hz was used. The spot diameter was 2.2 mm with a overlap rate of 50%. Both sides of the specimens were treated to achieve a stress balance. In this experiment, the laser power densities of 6.05 GW/cm^2, 6.58 GW/cm^2 and 7.37 GW/cm^2 were used corresponding to the laser energies of 4.6 J, 5.0 J and 5.6 J respectively. A water curtain with the thickness of about 2 mm was utilized as transparent confining layer, while a professional aluminum foil with the thickness of 0.1 mm was used as absorbing layer to avoid thermal effects.

2.3 Fatigue test

Fatigue tests were performed in load-control mode on a MTS 809 servo-hydraulic machine with a load capacity of 250 kN at both room temperature in air (25 ℃) and high temperature of 600 ℃, 700 ℃ and 800 ℃. The fatigue apparatus is shown in Fig.2. A high-temperature furnace(MTS653) which ranged from +100 ℃ to +1400 ℃ was used to heat the specimen.
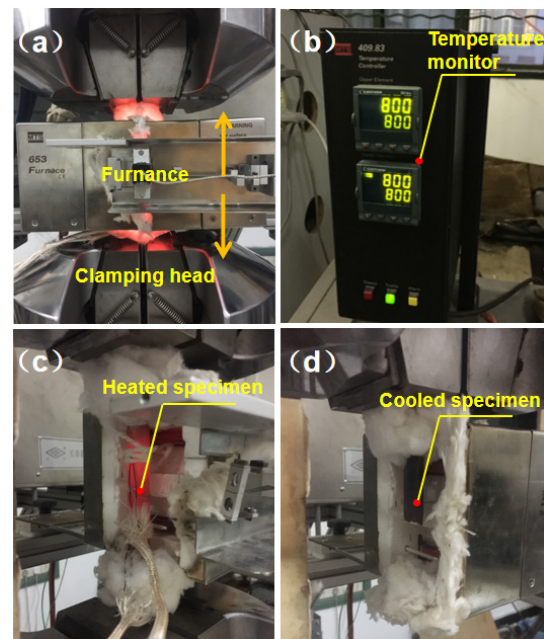
Fig.2 Specimen during high temperature fatigue and after cooling （a）High temperature furnace （b）Temperature-control device （c）Hot fracture （d）Cool fracture

The test frequency was 15 Hz, and the load ratio *R* was 0.1. We adopted an initial stress value of 330 MPa on the specimens. Five specimens were used for each test parameter. All the results have been at least duplicated and averaged to give a good statistical representation of the results. After fatigue test, the upper and lower fractures were released and ultrasonic cleaned for subsequent testing.

2.4 Microstructural observations

The surface grain structure near the fracture was observed in our research, the observation equipment was Keyence VHX-1000 digital microscope, the corrosive solution used was 500 mL HCL, 35 mL H_2SO_4, 150 g $CuSO_4$, and the corrosion time was 30 s. Surface microstructures of the non-LPed and LPed specimens were characterized by a JEM-2100 transmission electron microscopy (TEM) which was operated at a voltage of 200 kV. TEM thin foils were obtained from top surface of the specimens. Each TEM thin foil was mechanically polished to the thickness with 150 μm from the side opposite to the treated surface, followed by dimpling and ion milling from that side to observe the microstructural changes close to the very top surface (< 20 μm).

3. Results and discussion
3.1 High-temperature fatigue life
3.1.1 Effects of laser power density on fatigue life

Comparison of fatigue life between LPed specimens and untreated specimens at different temperatures is shown in Fig.3.
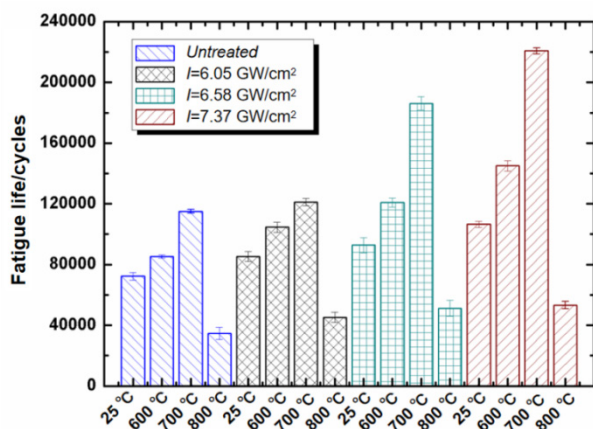

Fig.3 Comparison of fatigue life between LPed specimens and untreated specimens at different temperatures.

It can be seen from Fig.3 that the fatigue life of the LPed specimens is significantly improved compared to the untreated specimens. The fatigue life of untreated specimen was 7.23×10^4 cycles at room temperature (25℃). However the fatigue lives of LPed specimens are 8.53×10^4, 9.28×10^4 and 10.65×10^4 cycles corresponding to the laser power density of 6.05 GW/cm², 6.58 GW/cm² and 7.37 GW/cm² respectively, which are increased by 18.0%, 28.5% and 47.4% respectively. Some previous researches showed that the depth of CRS in the subsurface of service parts was a key factor that affecting their service lives [31-32]. Hammersley et al. [33] claimed that the affected layer depth of IN718 alloy treated by LP could reach 1.2 mm, while this value was

only 0.3 mm after shot peening. The subsequent results of high-cycle fatigue test further verified that the LP could gain a maximum fatigue life of 140% compared to the untreated one. The grain refinement and generation of high density of dislocation induced by LP are also crucial to the enhancement of fatigue life [34-35]. The denser surface effectively inhibits the initiation and propagation of cracks, thus improve the fatigue resistance of IN718 alloy. What's more, it is observed that with the increase of laser power density, the fatigue life of the specimen also increases. In particular, the fatigue life is increased by nearly 47.4% compared with the untreated specimens under the laser power density of 7.37 GW/cm². The results show that the LP process with reasonable laser power density can improve the gain effect of the fatigue resistance significantly.

3.1.2 Effects of temperature on fatigue life

Fig.3 also shows that the fatigue lives of the specimens fluctuate greatly at high temperatures. For untreated specimens, the fatigue lives are increased by 18.0% and 59.3% at 600 ℃ and 700 ℃ while compared with that at room temperature. However when the temperature increases to 800 ℃, the fatigue life drops suddenly, which is 52.0% lower than that at room temperature. This phenomenon also occurs in the specimens treated by LP. For the LPed specimen with a laser power density of 6.05 GW/cm², the fatigue lives are increased by 22.7% and 42.0% at 600 ℃ and 700 ℃ while compared with that at room temperature. However when the temperature increases to 800℃, the fatigue life drops suddenly, which is 46.9% lower than that at room temperature. For the LPed specimens with a laser power density of 6.58 GW/cm², the fatigue lives are increased by 30.2% and 100.5% at 600 ℃ and 700 ℃ while compared with that at room temperature. However when the temperature increases to 800 ℃, the fatigue life is 44.8% lower than that at room temperature. For the LPed specimens with a laser power density of 7.37 GW/cm², the fatigue lives are increased by 36.2% and 107.3% at 600 ℃ and 700 ℃ while compared with that at room temperature. However when the temperature increases to 800 ℃, the fatigue life is 50.0% lower than that at room temperature. To sum up, temperatures of 600℃ and 700 ℃ are beneficial for improving the fatigue life of both LPed and untreated specimens, while higher temperature 800 ℃ may lead to deterioration of fatigue performance.

3.2 Microstructures after high-temperature fatigue tensile

In order to analyze the morphological change of grains before-and-after fatigue tensile, the fractures of untreated and LPed specimens after fatigue tensile at both room and high temperature (*T*=700 ℃) were observed respectively. The metallographic analysis is shown in Fig.4.

It is noted that the grain size of the fracture in Fig.4(a) has increased to a certain extent after fatigue tensile while compared with the specimen before fatigue tensile. The relevant theories of metallurgy exhibits that the deformation energy and the applied mechanical energy can drive the grain size to increase [36]. On the one hand, due to the occurrence of plastic deformation during the process of fatigue tensile, crystal defects, such as dislocation, will be generated substantially inside the grains. Then the crystal defects will

lead to lattice distortion of the grains and greatly increase the energy inside the grains, causing the grains to grow. On the other hand, due to the applied loading, the twin boundary in the grains will move, and the small-angle grain boundary undergo cyclic reciprocating movement under external loading. However, the anisotropic elastic modulus of the grains will change the atomic energy of different grains, which causes the grains to move.
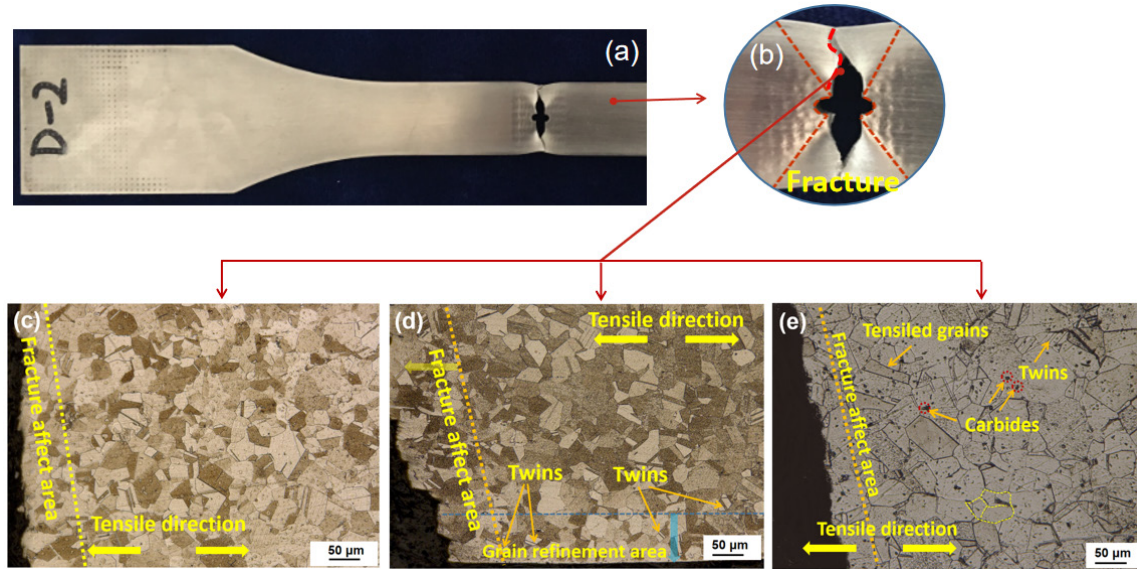
Fig.4 (a) Morphology of fatigue fracture, (b) Enlarged view of fracture, (c) Fracture of untreated specimen at room-temperature, (d) Fracture of LPed specimens at room-temperature and (e) Fracture of LPed specimens at the temperature of 700°C（*I*=7.37 GW/cm^2）.

Comparing with Fig.4(c) and Fig.4(d), we can conclude that the grain morphology of the affected zone of fracture after LP was slightly different with that before LP. The grains in the fracture affected area of untreated specimens were orderly, while the grains in the fracture surface of LPed specimens were disorderly and finer. These fine and randomly distributed grains will hinder the growth of crack, reduce the crack growth rate, and improve the fatigue life.

The shear force required for crack initiation can be expressed as:

$$\tau_N = (\frac{2Gv_m}{D})^{-\frac{1}{2}} \tag{1}$$

Where G is the shear modulus, v_m is the effective surface energy of crack, and D is the grain size. From the Eq.(1), it is known that the τ_N decreases with the increase of grain size, the larger the grains are, the easier it is to crack. At the same time, with the increase of grain size, the number of trigeminal grain boundary decrease, as a result, the crack growth will encounter less obstacles in the crack growth process, results in the decrease of crack growth resistance. On the contrary, if the grain size decreases, the contribution of grain boundary sliding to deformation increases, so that the crack tip is passivated, the rate of deformation increases, and the crack growth rate decreases [37]. Therefore, our research well explained the reason why the fatigue life of the LPed specimens is higher than that of the untreated specimens at room temperature.

On the other hand, from Fig.4(d) and Fig.4(e), it can be found that the grain size after fatigue tensile at high temperature is increased significantly compared with that at room temperature. In addition, a large amount of precipitated particles, including γ''-precipitate and γ'-precipitate are evenly dispersed in the grain interior and on the grain boundary, forming a coherent relationship with the matrix(γ-precipitate), so as to achieve the strengthening effect on the IN718 alloy. Even at high temperature, the effect of coherent strengthening still exists. Some carbides are dispersed in the grains as shown in Fig.4(e). These carbides play a role in hindering the free movement of dislocation during plastic deformation and generating work-hardening which reduces the probability of crack initiation effectively and delay the occurrence of microcracks.

3.3 Microstructural characteristics of specimens before-and-after high-temperature fatigue tensile
3.3.1 Analysis of dislocation configuration before-and-after LP

In order to further explore the microscopic dislocation configuration of IN718 alloy induced by LP and its evolution at high-temperature, the surface structure of untreated, LPed specimens at room and high temperature (700 °C) were carried out by TEM observation, the TEM results is shown in Fig.5.

Fig.5(a) shows clear grain boundary and grain structure, the grains are fine and uniform. After LP treatment, the grain size is decreased as seen in Fig.5(b), and in some specific regions, twin region with the same direction appeared, and the distance between the twins was almost equal. It is well known that the CRS induced by LP can hinder the initiation and propagation of fatigue cracks and improve the fatigue properties of material. The CRS is often the result of microplastic deformation and microstructural changes [38-39]. Therefore, it can be reasonably assumed that one of the reasons of the effect of structure strengthening in IN718 alloy

induced by LP is the mixed effect of twin structure and dislocation.
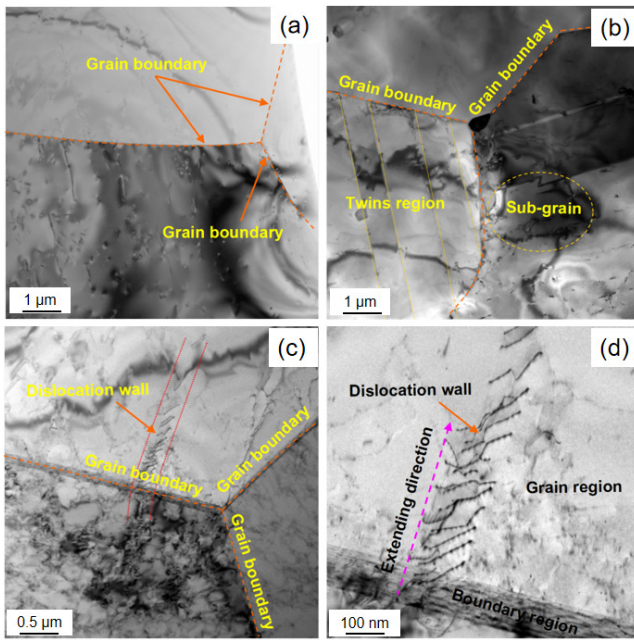
Fig.5 TEM figures on the top surface of different specimens. (a) Untreated, (b) LP treated （I=7.37 GW/cm^2）, (c) LP treated + heat exposure and (d) Local amplified view of Fig.5(c).

The distance between twins is closely related to the size L of the refined structure and is a function of shear stress τ (Eq.(2)):

$$L = 10Gb/\tau \qquad (2)$$

Where G is the shear modulus, b is the Burgers vector [40]. Obviously, the magnitude of shear stress directly affects the spacing between the twin striation. The smaller the spacing of twin striation, the finer the microstructures formed by interweaving dislocation. The visualized structure of subgrains has appeared in Fig.5(b), and the refined grains are direct reason for improving the fatigue resistance of IN718 alloy. Fig.5c is the grain configuration of the LPed specimens after heat exposure, and Fig.5(d) is an enlarged figure of its characteristic region.

It can be seen from Fig.5(c) that the dislocations are slipping and climbing under high temperature, and the dislocation develops in a direction from the grain boundary to the inside of the grains, then forms a unique "array" region. These transgranular dislocation arrays interact with the grain boundary, and then inhibits the growth of grain boundary to a certain extent. The above phenomenon also explains the fundamental reason why the grain size of the LPed specimens after heat exposure is still smaller than the size of substrate. On the other hand, the enhancement of dislocation activities consumes a large amount of stacking-fault energy, which weakens the power of grains growing. This is also an important factor to suppress grains coarsening. At the same time, the high temperature promotes the development of dislocation from the high-energy state to the low-energy state. The dislocation tangles expand gradually, and the dislocation

density tends to decrease. Therefore, the dislocation density will decrease with time at 700 ℃ .

3.3.2 Microstructures of high-temperature fatigue specimens under different laser power densities

(1) Microstructures of grain boundary near the fatigue fracture

Since the grain boundary is an extremely important region during the process of high-temperature fatigue, so the microstructure at the typical grain boundary is first observed. It is found from Fig.6 that there are a large number of different dislocation structures distributed around the grain boundary at 700 ℃. As shown in Fig.6(b,c,d), the dislocation density in the LPed specimens is greater than that in the untreated specimens. Most of the dislocation movement results in dislocation pile-up at grain boundary, and larger laser power density leads to more severe dislocation pile-up.
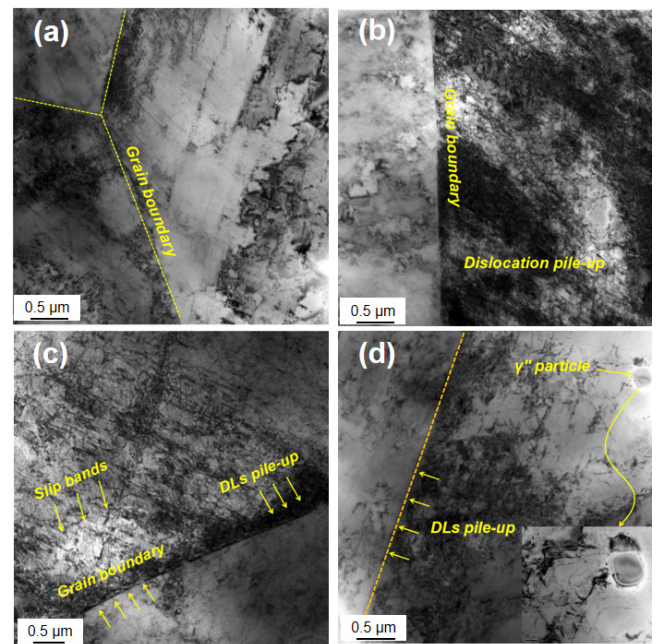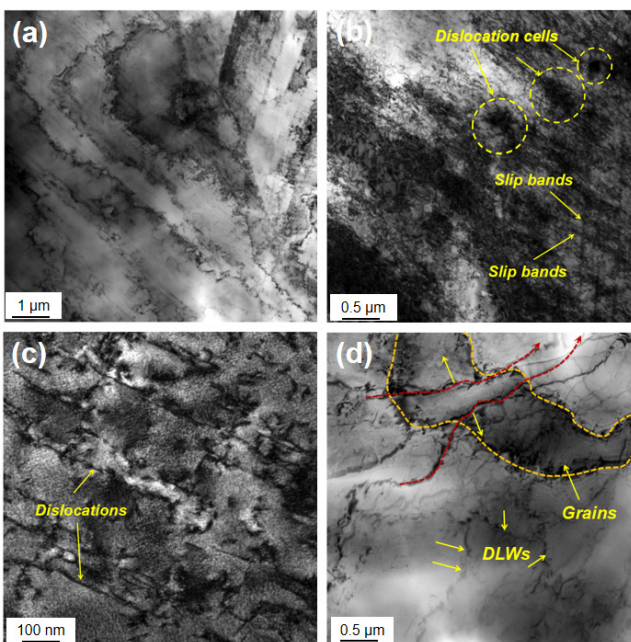

Fig.6 Microstructures around the grain boundary in the subsurface of specimens after fatigue at 700 ℃.(a)Untreated, (b) I=6.05 GW/cm^2, (c) I=6.58 GW/cm^2 and (d) I=7.37 GW/cm^2.

In fact, the grain boundary acts as an obstacle during the dislocation movement. When the dislocation moved to the grain boundary, it is easy to gather around the grain boundary. As the process of deformation continues, the new dislocation will continue to gather and the dislocation pile-up is formed eventually. In particular, the particles of γ'' strengthened phase with a size of about 250 nm are found in the LPed specimens with laser power density of 7.37 GW/cm^2. As shown in Fig.6(d), many dislocation are gathered around the γ'' strengthened phase. In addition to the coherent distortion of the matrix, the γ'' strengthening phase can also interact with the movement of dislocation, hindering the movement of dislocation effectively, which helps to reduce the process of plastic deformation and reduce the fatigue crack growth rate.

(2) Microstructures inside grains near the fatigue fracture

In order to reveal the effect of dislocation movement on high-temperature fatigue properties, the characteristics of

dislocation movement inside the grains were observed. In Fig.7(a), the dislocation distribution of the untreated specimens is more dispersed and uniform, the dislocation density is lower than that of the LPed specimens. However, within the grains of the LPed specimens, the configuration of dislocation is more complicated, and the interaction between the dislocation is more obvious. The obvious structure of dislocation cells and a certain number of dislocation slip bands can be seen in Fig.7(b). In particular, the dislocation slip bands exhibit multi-directional characteristic. According to the analysis, the strong plastic deformation of the material surface leads to a unidirectional slip bands in the process of LP. Then the subsequent plastic deformation during the process of fatigue tensile forms a slip bands in the another direction. The density of the dislocation line is higher than that of the untreated specimens significantly in Fig.7. In addition, the structure of dislocation walls(DLWs) can be observed in Fig.7(d).
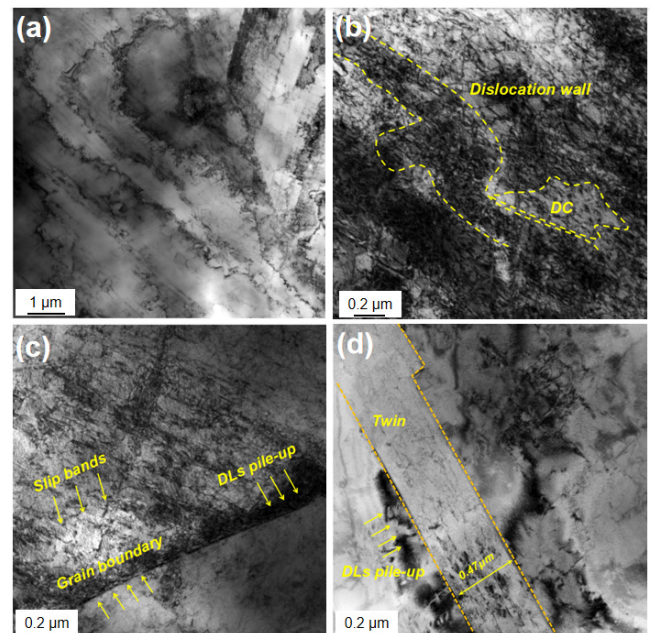

Fig.7 Microstructures inside grains in the subsurface of specimens after fatigue at 700 °C. (a)Untreated, (b) I=6.05 GW/cm^2, (c) I=6.58 GW/cm^2 and (d) I=7.37 GW/cm^2.

Although the material surface will produce slippage proliferation of dislocation after LP, the slippage of these dislocation is incomplete. The original structure of dislocation will move and slip, when the material treated by LP undergo high-temperature and plastic deformation of cyclic loading again. And the slip dislocation will form dislocation walls and dislocation cells through the rearrangement in the process of continuous tangling and climbing. It can also be found in Fig.7(d) that the dislocations cross the grain boundary and divide the original grains twice in some irregular grains. As we all know, the dislocation within the grains will encounter different obstacles when it moving, and the grain boundary is an important factor hindering its movement. At low temperatures, the dislocation will slip across the barrier, only when the applied stress is greater than the internal stress caused by the barrier. At high temperature, the process of thermal activation is more active, and it is easier for the dislocation to cross these barriers under thermal activation. As the power density of LP increases, the coupling effect of external stress and thermal activation assists dislocation slip through grain boundary smoothly. In summary, the dislocation structure of the specimens with the combined action of high-temperature and cyclic loading after high-temperature fatigue tensile is more complicated than the specimens before high-temperature fatigue tensile, and the number of dislocation increases significantly.

(3) Twin structures inside grains near the fatigue fracture

Twins is another important form in the plastic deformation of IN718 alloy. The dislocation configuration analysis of IN718 alloy after LP shows that the deformation twins with same direction have been found in some specific regions. The width of these twins is about 1 μm, and the interweaving of twins and dislocation play a certain role in the refinement of grains. In the LPed specimens with laser power density of 7.37 GW/cm^2, some twin striation with a width of about 0.47 μm are observed even at high temperature, as shown in Fig.8(d).

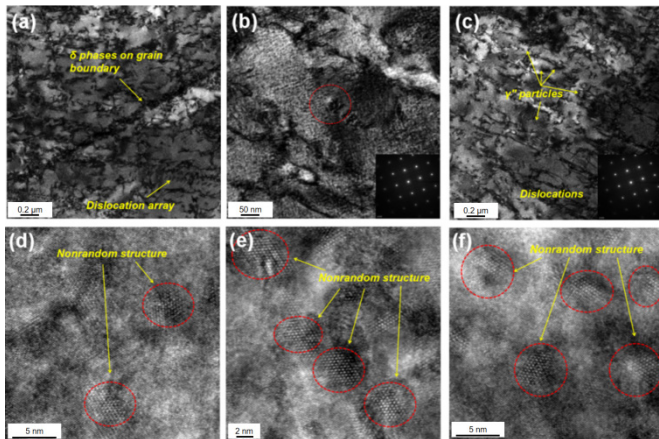**Fig.8** Twins inside grains in the subsurface of specimens after fatigue at 700°C.
(a) Untreated, (b) I=6.05 GW/cm^2, (c) I=6.58 GW/cm^2 and (d) I=7.37 GW/cm^2.

It is worth noting that the observed twin striation show the morphology of wide at the top and narrow at the bottom. It can be speculated that the stress in the mechanical twins is much greater than the stress of the surrounding matrix, and causing the band structure to deform. The width of the twins at high temperature is smaller than that at room temperature, which shows that the number of twins will gradually decrease as the temperature continues to increase. Then the dislocation gradually change from dislocation lines(DLs) and dislocation tangles to dislocation walls, dislocation cells(DCs) and other structures, and become the main microstructure in fatigue fractures eventually. Of course, in our research, we only found the twin structure in the LPed specimens with laser power density of 7.37 GW/cm^2, but no trace of twins was found in the specimens treated by LP with low power density, which is related to the degree of plastic

deformation induced by high-pressure shock-wave and the magnitude of strain rate. Usually, the greater the strain rate is, the easier it is to form twins during the plastic deformation. Because with the increase of strain rate, the plastic deformation methods such as cross-slip and the slip of grain boundary are difficult to proceed, resulting in local stress concentration, then promoting the production of twins. The LP with high power density is often accompanied by a higher strain rate, and it is easier to promote the formation of twin structures, which explains the reason reasonably why the twin striation appear only in the LPed specimens with laser power density of 7.37 GW/cm^2. Of course, the twins introduced by early plastic deformation have an important influence on the subsequent mechanical behavior of the alloy, which can adjust the orientation of grains, then improving the high-temperature mechanical properties of the material.

(4) Precipitates inside grains near the fatigue fracture

Fig.9 exhibits precipitates inside grains in the subsurface after LP at different laser power densities under 700℃. From Fig.9, it is noted that there were different dislocations and precipitates inside grains of LPed specimen. Among them, long δ-precipitate was found in the LPed specimens with a laser power density of 6.05 GW/cm^2, which was formed by the secondary growth and transformation of the strengthening γ"-precipitate at high temperature. The previous researches have shown that a small amount of δ-precipitate can improve the resistance of intergranular crack propagation, and transform intergranular fracture at high temperature into a mixed fracture mode of intergranular and transgranular [41].

Fig.9 Precipitates inside grains in the subsurface of LPed specimens after fatigue at 700 ℃.
(a) I=6.05 GW/cm^2, (b) I=6.58 GW/cm^2, (c)I=7.37 GW/cm^2, (d) HR-TEM of Fig.9(a), (e) HR-TEM of Fig.9(b) and (f) HR-TEM of Fig.9(c).

A small amount of δ-precipitate distributed along the grain boundary can also become an obstacle to slippage, and hinder the movement of dislocation during plastic deformation eventually, thus generating dislocation pile-up, and reducing the relaxation rate of CRS. However, with the temperature continues to increase, a large amount of δ-precipitate precipitates and grows, which will reduce the number of strengthening γ"-precipitate with coherent distortion. The large δ-precipitate is prone to embrittlement and crack under the effect of external stress, forming a crack source.

Therefore, the researchers often try to increase the dissolution temperature of γ"-precipitate and γ'-precipitate to hinder the transition from γ"-precipitate to δ-precipitate in the development of a new type of IN718 alloy. This method can change the precipitation behavior of γ"-precipitate and γ'-precipitate and improve their stability. In addition to the coarsening δ-precipitate, a large number of randomly distributed γ"-precipitate can be seen in Fig.9(c), which are entangled with a large number of dislocation to form a unique entanglement of "dislocation-precipitate". The unique entanglement is helpful to further pinning the moving dislocation to form dislocation entanglements with higher density at high temperature. Further more, high-power TEM showed that the number of ordered structure is different under the different laser power density, especially, the number of ordered atomic arrays is larger at high laser power.

3.3.3. Microstructural characteristics of fatigue specimens at different temperatures

(1) Microstructures of grain boundary near the fatigue fracture

As can be seen in Fig.10, a large number of dislocation structure are found in the fatigue fracture at both room and high temperature, and the dislocation density is much higher than that before high-temperature fatigue tensile. The dislocations are proliferated with the development of plastic deformation and move along with the direction of stress under the action of fatigue loading. However, when the dislocations move to the grain boundary, they are hindered by the grain boundary and quickly accumulated around the grain boundary, forming temporary stress concentration. The phenomenon of dislocation pile-up around the grain boundary was observed at each temperature in the Fig.10. However, the degree of dislocation pile-up is more obvious at 600 ℃ and 700 ℃, as shown in Fig.10(b, c). This is probably because the high temperature activates the dislocation movement better, making it more active under the same stress of external loading. Of course, some previous researches also believed [42] that the change of high-temperature sliding mode is one of the important reason for changing the fatigue properties of IN718 alloy. For example, part of the plane sliding is transformed into wavy sliding in the free precipitation state, as a result, a more evenly distributed slip region is formed, which allows the material to harden and increase its fatigue life. However, the fatigue properties of the material does not increase infinitely with the increase of temperature. Macroscopic fatigue properties has shown that the fatigue properties of IN718 decreased significantly at 800℃, as shown in Fig.3. Although the dislocation pile-up in Fig.10(d) is still obvious, but the growth of grains, the weakening of grain boundary, and the coarsening and recovery of precipitate are important factors to reduce the high-temperature mechanical properties of the material at 800 ℃.
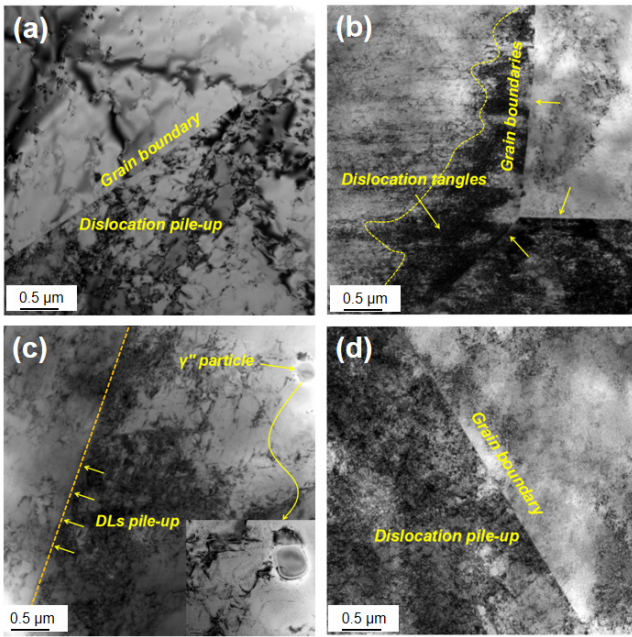
Fig.10 Microstructures near grain boundary in the subsurface of LPed specimens (I=7.37 GW/cm^2) after fatigue at different temperatures.
(a) Room temperature, (b) T=600 °C, (c) T=700 °C and (d) T=800 °C.

(2) Microstructures inside grains near the fatigue fracture

It is generally believed that there are two main reasons for the increase of fatigue resistance of LPed specimens at high temperature. One is that high-amplitude CRS induced by LP. Another is that stable micro-strengthening structures are formed, including high density of dislocations, dislocation tangles and the significantly increased slip bands.

In Fig.11, typical substructures like dislocation tangles, the ordered combination of dislocation walls, and subgrains (Fig.11(c)) are observed. These substructures are stable even at high temperature.

In theory, the grain size can be reduced or the dislocation density can be increased by plastic deformation, then improving the strength of solid solution and the degree of precipitation hardening of the alloy [43].

$$\sigma_f = \sigma_0 + \sigma_{sss} + \sigma_{ppt} + kd_{fp}^{-\frac{1}{2}} + \alpha Gb\rho^{-\frac{1}{2}} \quad (3)$$

Where σ_f is the strength, σ_0 is the friction stress, σ_{sss} is the stress of solid-solution strengthening, σ_{ppt} is the stress of precipitation strengthening, k is the Hall-Petch constant, d_{fp} is the average free travel of dislocation, α is the constant, G is the shear modulus, b is the burgers vector, ρ is the dislocation density. The first three terms ($\sigma_0 + \sigma_{sss} + \sigma_{ppt}$) in the Eq.(3) are constants. Therefore, the solid-solution strength of the material is positively related to the dislocation density. In our research, the material can still maintain a high dislocation density even at high temperatures, which is an important factor for the excellent fatigue properties of IN718 alloy at high temperatures, especially at 700 °C.
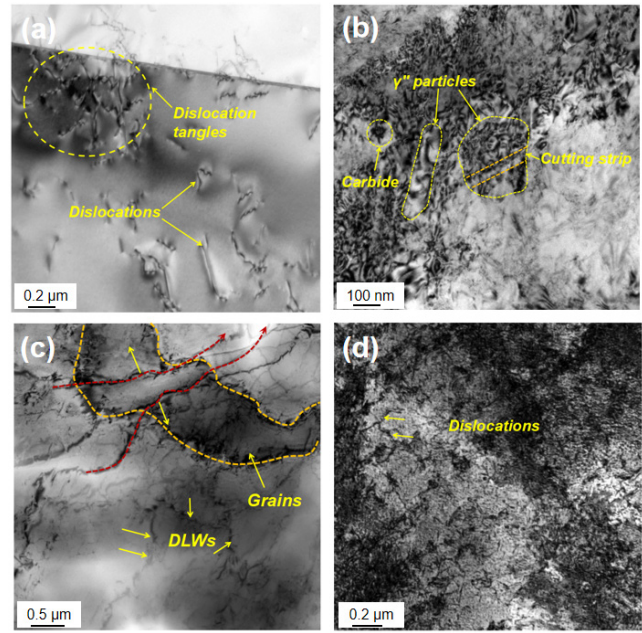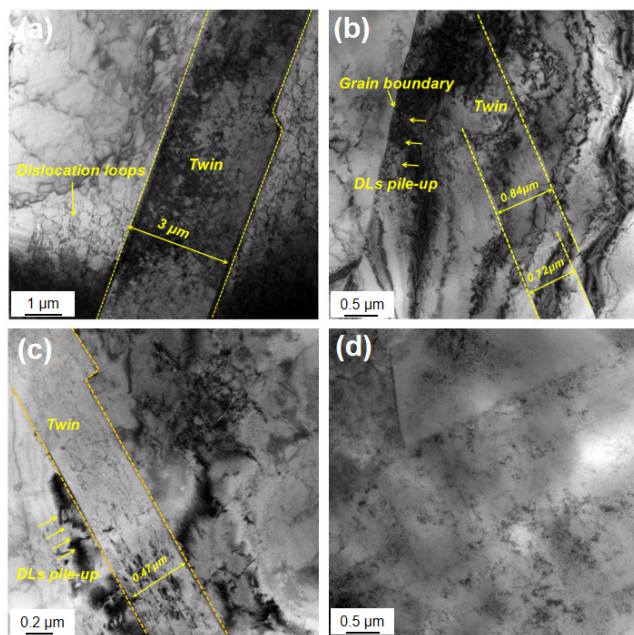

Fig.11 Microstructures inside grains in the subsurface of LPed specimens(I=7.37 GW/cm^2) after fatigue at different temperatures. (a)Room temperature, (b) T=600 °C, (c) T=700 °C and (d) T=800 °C.

Many previous researches [44-45] have reported that the fatigue life of nickel-based alloy under high temperature has increased compared with that under room temperature. These researches suggested that the γ"-precipitate is activated by the cross-slip mechanism when the temperature increases, which greatly increases the effect of dislocation pinning. The strengthening of γ"-precipitate also increases the precipitation strengthening stress σ_{ppt} at high temperature, which better hinders the deformation of single dislocation slip region. The slip mode is changed from plane slip to wave slip when the temperature rises, which makes the distribution of slip region more uniform, and the fatigue life of the material will also increase.

(3) Twin structures inside grains near the fatigue fracture

Fig.12 shows the twin structures inside grains near the fatigue fracture at different service temperatures when the laser power density is 7.37GW/cm^2.

It can be seen from the figure that the twin structures with clear outline are found in the specimens at room temperature, 600 °C and 700 °C. It is consistent that the morphology of the twins is deformed, then shows a morphology of narrow at the top and wide at the bottom, which indicates that the internal stress of the twins is much greater than that of the surrounding matrix material. The width of twins varies from 0.47 μm to 3 μm, the largest width is the twins at room temperature with a width of 3 μm, and the smallest width is the twins at 700 °C with a width of 0.47 μm. When the temperature increases to 800 °C, the twins disappeared basically. With the increase of temperature, the scale of twins showed a trend of decreasing gradually. Therefore, the number and width of the mechanical twins are closely related to the temperature.

Fig.12 Twin structures inside grains near the fatigue fracture of LPed specimens (I=7.37 GW/cm^2) at different service temperatures .(a) room temperature, (b) T=600 °C, (c) T=700 °C and (d) T=800 °C.

At room temperature, the twins with large-scale structure will become an obstacle to the movement of dislocation. In particular, the twin boundary works like the grain boundary. When the dislocation moved to the twin boundary, they will accumulate and form stress concentration. At 600 °C and 700 °C, the width of twins is smaller than that at room temperature, as shown in Fig.12(b, c). But at the same time, the dislocation density did not decrease, and the distribution of dislocation structure is more uniform. With the temperature increases, the activation energy of the slip system decreases gradually, the dislocation activities became easier, and the dislocation slip dominates the entire deformation process. When the service temperature increases to 800 °C, the mechanical twins disappear gradually, and the dislocation pile-up is difficult to achieve. Finally, the dislocation disperses in the grains, as shown in Fig.12(d). On the one hand, the existence of twin boundary is an obstacle to the movement of dislocation, on the other hand, it is an important factor for the refinement of grains. Under the combined action of high thermal activation energy and cyclic loading, the movement of dislocation and the proliferation of new dislocation lead to a large number of dislocation tangles, then forming dislocation walls and dislocation cells gradually. These new dislocation structure and twin interweave to form a series of new grain boundary, and divide the original coarse grains into smaller grains gradually. Therefore, the appearance of twin structure not only has a certain resistance to the plastic deformation in the fatigue process, but also change the original distribution system of grains, then forming more stable structure of subgrains, and improving the high-temperature fatigue characteristics of the material effectively.

(4) Precipitates inside grains near the fatigue fracture

The high-temperature precipitate of the specimens at different temperatures was characterized by TEM, as shown in Fig.13. It can be seen from the figure that the high-

temperature precipitate of the specimens is mainly the ordered γ"-precipitate at 600 °C and 700 °C, while the high-temperature precipitate is mainly the coarsened δ-precipitate particles at 800 °C. The different precipitates has great influence on the slip characteristics of IN718 alloy during high-temperature fatigue. First of all, the influence of γ"-precipitate with different size on the relative slip characteristics is different significantly. The previous researches have shown that compared with the microstructure of larger γ"-precipitate, the microstructure of smaller γ"-precipitate showed more obvious multi-system slip-tendency [46]. Compared Fig.13(a) with Fig.13(b), it can be seen that the size of γ"-precipitate at 600 °C is slightly smaller than that at 700 °C, so the γ"-precipitate at 600 °C has more and more dense slip bands. The denser and longer the region of slip bands is, the plastic deformation of alloy is more serious. In addition, too many slip bands are easy to cut the strengthening γ"-precipitate and make it lose the ordered structure, thus losing the coherent relationship with the matrix γ-precipitate, and reducing the strengthening effect on the matrix finally.

Of course, the interaction between the γ"-precipitate and the growing dislocation will form local dislocation pile-up in some special regions, such as grain boundary, twin boundary and carbide. The local dislocation pile-up will hinder the movement of dislocation, then forming the hardening effect of these regions. The local dislocation pile-up also conducive to reduce the probability of fatigue crack initiation in the process of high-temperature fatigue, then slowing down the fatigue crack growth rate , and extending the fatigue life of service parts.
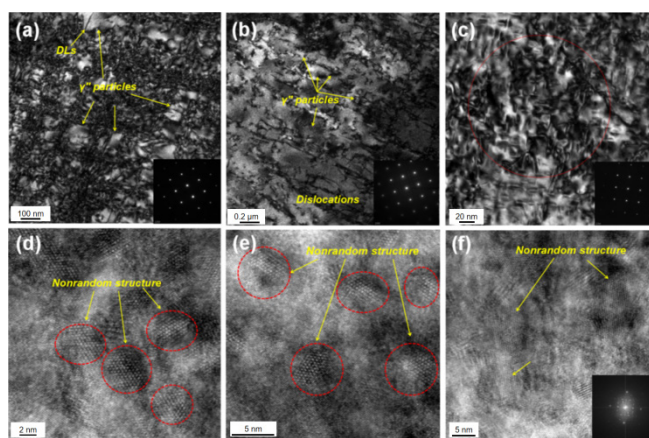
Fig.13 Precipitates inside grains near the fatigue fracture of LPed specimens (I=7.37 GW/cm^2) at different service temperatures. (a)T=600 °C, (b) T=700 °C, (c) T=800 °C, (d) HR-TEM of Fig.13(a), (e) HR-TEM of Fig.13(b) and (f) HR-TEM of Fig.13(c).

However, the original precipitated strengthening γ"-precipitate are coarsened and transformed into δ-precipitate gradually when the temperature increases to 800 °C, as shown in Fig.13(c). But too much δ-precipitate will reduce the coherent distortion of γ"-precipitate and reduce the high-temperature fatigue performance of the material. In addition, it can also be observed from high-power TEM that the number of steady-state nanostructures are decreased with the increase of temperature at 800 °C. In conclusion, the relatively stable strengthening precipitate can be obtained near 700 °C in IN718 alloy, which help to improve the high-temperature fatigue performance of the specimens. The number of

beneficial precipitates decrease with the increase of temperature, and the high-temperature fatigue life of the specimens decreases accordingly.

4. Conclusion

The microstructures of IN718 treated by LP after high-temperature fatigue tensile, and the microstructural characteristics before-and-after high-temperature fatigue tensile were characterized in detail by using transmission electron microscopy (TEM). The microstructural characteristics before-and-after high-temperature fatigue tensile include the microstructure in surface grain boundary region and inside grains near the fatigue fracture, also include the twin structure and high-temperature precipitates inside grains near the fatigue fracture. The main conclusions are as follows:

(1) The TEM results showed that a large number of dislocations were deposited near the grain boundary of the material in the high-temperature fatigue fractures, and the degree of the deposition was increased with the increase of the laser power density. A variety of new dislocation structures, such as dislocation walls and dislocation cells, were formed in the grains of the LPed specimen after high-temperature fatigue. The interaction between these structures and the original dislocations was an important reason to improve the local working hardening and the high-temperature fatigue properties of the material. The structure of mechanical twins in the high-power LPed specimens can adjust the grain orientation, and the interaction with other dislocation structure can refine the coarse grains to a certain extent. However, the twin boundaries were disappeared gradually at 800 ℃, and the degree of dislocation pile-up was smaller than that at 600 ℃ and 700 ℃.

(2) The special "dislocation-precipitate" entanglement among the strengthening particles of γ''-precipitate and a large number of dislocations in the high-temperature fatigue specimens at 700 ℃ was helpful to form a more effective pinning of the dislocation movement and the effect of hardening. The entanglement was beneficial to prevent the initiation and propagation of fatigue cracks. However, the coarsened δ-precipitate at 800 ℃ reduced the coherent distortion of γ''-precipitate and reduced the high-temperature fatigue properties of the material.

References

[1] D. Dudzinski, A. Devillez, A. Moufki, D. Larrouquere, V. Zerrouki, and J. Vigneau: Int. J. Mach. Tool. Manu., 44, (2004) 439.

[2] M. Nalbant, A. Altin, and H. Gokkaya: Mater. Design., 28, (2007) 1334.

[3] J. Sheng, S. Huang, J.Z. Zhou, and Z.W. Wang:Eng. Fract. Mech., 169, (2017) 99.

[4] W.K. Deng, J.H. Xu, Y.M. Hu, Z.W. Huang, and L. Jiang:Mater. Sci. Eng. A., 742, (2019) 813.

[5] C.H. Pei, D. Shi, H. Yuan, and H.X. Li:Mater. Sci. Eng. A., 759, (2019) 278.

[6] C. Duan, X.H. Chen, and R.W. Li: A. S., 3, (2020) 87.

[7] G. M. D. Almaraz, M. G. Tapia, and A. Dominguez: Procedia. Struct. Integr., 26, (2020) 20.

[8] S.Q. Xu, S. Huang, X.K. Meng, J. Sheng, H.F. Zhang, and J.Z. Zhou: Opt. Laser. Eng., 94, (2017) 70.

[9] S. Huang, M.X. Liu, X.Q. Hu, H.Y. Li, and L. Hu: J. Drain. Irrig. Mach. Eng., 37, (2019) 730.

[10] S. Kim, H. Choi, J. Lee, and S. Kim:Int. J. Fatigue., 140, (2020) 105802.

[11] J.Z. Zhou, Y. Han, S. Huang, X.K. Meng, J. Sheng, W.L. Zhu, and S.Q. Xu: Rare. Metal. Mat. Eng., 45, (2016) 1509.

[12] M. HoRnqvist, T. Mansson, and D. Gustafsson: Procedia. Eng., 10, (2011) 147.

[13] J. Belan, M. Matvija, L. Kucharikova, and E. Tillová:Mater. Today: proceedings., 5, (2018) 26697.

[14] Q. Hu:J. Mater. Eng. Perform., 8, (2012) 92.

[15] M. Schlesinger, T. Seifert, and J. Preussner: Int. J. Fatigue., 99, (2017) 242.

[16] J. Li, J.Z. Zhou, A.X. Feng, S. Huang, X.K. Meng, Y.J. Sun, Y. Huang, and X.L. Tian:Opt. Laser. Technol., 118, (2019) 183.

[17] R.K. Nalla, I. Altenberger, U. Noster, G.Y. Liu, B. Scholtes, and R.O. Ritchie:Mater. Sci. Eng. A., 355, (2003) 216.

[18] J.Z. Lu, H.F. Lu, X. Xu, J.H. Yao, J. Cai, and K.Y. Luo: Int. J. Mach. Tool. Manu., 148, (2020) 103475.

[19] S. Keller, M. Horstmann, N. Kashaev, and B. Klusemann:Eng. Fract. Mech., 221, (2019) 106630.

[20] J.Z. Zhou, Y.J. Sun, S. Huang, J. Sheng, J. Li, and E. Agyenim-Boateng: Opt. Laser. Technol., 109, (2019) 263.

[21] J. Li , J.Z. Zhou, A.X. Feng, Y. Huang, X.L. Tian, S. Huang, and X.K. Meng:Opt. Laser. Technol., 120, (2019) 105763.

[22] A.G. Samuel, X.D. Ren, L.E. Asuako, Y.P. Ren, and Z.P Tong:Opt. Laser. Technol., 108, (2018) 177.

[23] J. Sheng, H. Zhang , and X. Hu: Theo. Appl. Fract. Mec., 109, (2020) 102757.

[24] A.Gill, A.Telang, S.R.Mannava, D.Qian, Y.S.Pyoun, H.Soyama, and V.K.Vasudevan:Mater. Sci. Eng. A., 576, (2013) 346.

[25] L.Liu, J. Wang, and J. Zhou: Opt. Laser. Technol., 115, (2019) 325.

[26] J.Z.Lu, W.Q.Zhang, X.Jing, L.J.Wu, and K.Y.Luo: J. Laser. Appl., 29, (2016) 012007.

[27] A.S.Gill, A.Telang, C.Ye, S.R.Mannava, D.Qian, and V.K.Vasudevan:Mater. Charact., 142, (2018) 15.

[28] A.Telang, A.S.Gill, S.R.Mannava, D.Qian, and V.K.Vasudevan: Surf. Coat. Tech., 344, (2018) 93.

[29] M. Kattoura, S.R. Mannava, D. Qian, and V.K. Vasudevan: Int. J. Fatigue., 102, (2017) 121.

[30] Y.X. Geng, X. Dong, K.D. Wang, X. Yan, W.Q. Duan, Z.J. Fan, W.J. Wang, and X.S. Mei:Surf. Coat. Tech., 370, (2019) 244.

[31] M.A.S. Torres, and H.J.C. Voorwald:Int. J. Fatigue., 24, (2002) 877.

[32] M. Sticchi, D. Schnubel, and N. Kashaev: Appl. Mech. Rev., 67, (2015) 010801.

[33] G. Hammersley, L.A. Hackel, F. Harris:Opt. Laser. Eng., 34, (2000) 327.

[34] U. Trdan, M. Skarba, J. Grum:Mater. Charact., 97, (2014) 57.

[35] A. Salimianrizi, E. Foroozmehr, M. Badrossamay, and H. Farrokhpour:Opt. Laser. Eng., 77, (2016) 112.

[36] E.A. Loria: Pennsylvania: TMS, (1994) 649.

[37] S. Huang, J. Sheng, W.S. Tan, and Z.W. Wang: Acta.Optica.Sinica., 37, (2017) 233.

[38] X.C. Zhang, Y.K. Zhang, J.Z. Lu, F.Z. Xuan, Z.D. Wang, and S.T. Tu:Mater. Sci. Eng. A., 527, (2010) 3411.

[39] A. Belyakov, K. Tsuzaki, H. Miura, and T. Sakai:Acta. Mater., 53, (2003) 847.

[40] J.Z. Lu, K.Y. Luo, Y.K. Zhang, G.F. Sun, Y.Y. Gu, J.Z. Zhou, X.D. Ren, X.C. Zhang, L.F. Zhang, K.M. Chen, C.Y. Cui, Y.F. Jiang, A.X. Feng, and L. Zhang: Acta. Mater., 58, (2010) 5354.

[41] B.D. Hong, X.Yi, and Q.C. Meng: Acta. Metal. Sinica, 27, (1991):55.

[42] M. Kattoura, S.R. Mannava, D. Qian, and V.K. Vasudevan: Int. J. Fatigue., 104, (2017) 366.

[43] D. Hull, and D.J. Bacon: Phys. Today., 19, (1966) 91.

[44] M. Zimmermann, C. Stoecker, and H.J. Christ:Procedia Eng., 55, (2013) 645.

[45] A. Pineau, and S.D. Antolovich: Eng. Fail. Anal., 16, (2009) 2668.

[46] X. Yi, B.D. Hong, and Q.C. Meng:Mater. Mech. Eng., 1, (1991) 31.